Protein Science (1999), *8*:234–241. Cambridge University Press. Printed in the USA.

Identification of Tyr438 as the major in vitro c-Src phosphorylation site in human gelsolin: A mass spectrometric approach

VEERLE DE CORTE, HANS DEMOL, MARK GOETHALS, JOZEF VAN DAMME, JAN GETTEMANS, AND JOËL VANDEKERCKHOVE

Flanders Interuniversity Institute for Biotechnology, Department of Biochemistry, Faculty of Medicine, Universiteit Gent, Ledeganckstraat 35, B-9000 Ghent, Belgium

(RECEIVED July 9, 1988; ACCEPTED August 24, 1998)

Abstract

Gelsolin is an actin-binding protein (82 kDa) consisting of six repeated segments (S1–S6), each approximately 120 residues long. It interacts with phospholipids and we previously showed that phosphatidylinositol 4,5-bisphosphate promotes phosphorylation of gelsolin by the tyrosine kinase c-Src. We used a combination of different methods, such as thin-layer chromatography and anti-phosphotyrosine-agarose immunoprecipitation of phosphopeptides combined with matrix assisted laser desorption ionization-mass spectrometry (MALDI-MS) and post source decay (PSD) analysis, to identify the phosphorylation sites in gelsolin. The major phosphorylation site (Tyr438) was located in subdomain 4 (S4). Phosphorylation of gelsolin in the gelsolin-actin$_2$ complex was inhibited by 90%. Gelsolin phosphorylation by c-Src in the presence of lysophosphatidic acid also revealed Tyr438 as the most prominent site. Additional minor sites were found using the anti-phosphotyrosine bead immunoprecipitation method followed by MALDI-MS and PSD analysis. These sites, representing ~5% of the total phosphate incorporation, were identified as Tyr59, Tyr382, Tyr576, and Tyr624. Based on these results we generated antibodies which specifically recognize Tyr438 phosphorylated gelsolin.

Keywords: electrospray ionization mass spectrometry; gelsolin; matrix assisted laser desorption ionization–time of flight–mass spectrometry; post-source decay; thin-layer chromatography; tyrosine phosphorylation

Gelsolin is a widely distributed actin-binding protein that severs actin filaments and is also the founding member of a family of related actin-binding proteins consisting of a discrete number of segments (three or six) that display internal homology with each other (Vandekerckhove, 1990). Members include villin (Bretscher & Weber, 1979), adseverin (Maekawa et al., 1989), containing six segments each, and fragmin/severin from lower eukaryotes (three segments). In the presence of calcium, gelsolin binds two actin monomers. Addition of the calcium chelator EGTA to this gelsolin-actin$_2$ trimer releases one actin subunit at the reversible Ca^{2+}-dependent site. The EGTA-resistant gelsolin-actin complex caps the fast growing ends of filaments (so-called + ends) but has lost its severing activity (Janmey et al., 1985). Acidic phospholipids such as phosphatidylinositol 4,5-bisphosphate (PIP_2) dissociate gelsolin from filaments ends so that the filaments are free for polymerization (Janmey & Stossel, 1987). This mechanism lies at the basis of thrombin activation of platelets and associated changes in the actin cytoskeleton (Hartwig et al., 1995).

We recently described phosphorylation by c-Src of a group of actin-binding proteins interacting with PIP_2. Although phosphorylation in the absence of phospholipids was weak but detectable, a very strong induction of phosphate incorporation could be measured in vitro when the actin-binding proteins were incubated with PIP_2 (De Corte et al., 1997). This was found not only for gelsolin, but also for the capping protein CapG from macrophages and the ubiquitous G-actin sequestering protein profilin. Of all phospholipids tested, PIP_2 displayed the highest activity, resulting in a 25- to 30-fold increase in the phosphorylation rate. Interestingly, this effect was also observed to the same extent when lysophosphatidic acid (LPA) was present (Meerschaert et al., 1998). The latter ob-

Reprint requests to: Joël Vandekerckhove, Flanders Interuniversity Institute for Biotechnology, Department of Biochemistry, Universiteit Gent, Ledeganckstraat 35, B-9000 Gent, Belgium; e-mail: joel.vandekerckhove@rug.ac.be.

Abbreviations: DTT, dithiothreitol; ESI-MS, electrospray ionization-mass spectrometry; KLH, keyhole limpet hemocyanin; LPA, lysophosphatidic acid; MALDI-TOF-MS, matrix assisted laser desorption ionization–time of flight–mass spectrometry; PIP_2, phosphatidylinositol 4,5-bisphosphate; PSD, post-source decay; RP-HPLC, reverse phase–high performance liquid chromatography; SDS-PAGE, sodium dodecyl sulfate-polyacrylamide gel electrophoresis; 2D, two-dimensional; TFA, trifluoroacetic acid; TLC, thin-layer chromatography.

servation suggests that LPA may act as an intracellular modulator next to its known function as an extracellular agent, inducing changes in the actin cytoskeleton via a receptor-mediated signal transduction mechanism (Moolenaar et al., 1997). Phospho-peptide maps of gelsolin phosphorylated by c-Src either in the presence of PIP_2 or LPA suggested that both compounds enhance phosphorylation of the same residues, although these sites were so far not located in the primary structure (Meerschaert et al., 1998).

To obtain better insight in the potential role of phosphorylation of these proteins, we located the phospho-tyrosine residues in gelsolin through a combination of several protein chemical methods. One major site (Tyr438) and four minor sites were identified. The latter could only be identified through MALDI-mass spectrometry.

Results

Tyr438 is the major phosphorylation site in human gelsolin

We followed two strategies in identifying the positions of the phosphotyrosine residues. The first consisted of a conventional approach in which a tryptic peptide mixture, derived from ^{32}P-labeled phosphogelsolin, was passed over a reverse-phase column. Twenty percent of the eluate was analyzed on line by ESI-MS, while the remaining part was collected for further characterization, following peptide detection by UV absorbance at 214 nm. Selected peptides of interest were sequenced by Edman degradation.

In the second approach a similar digest was separated by 2D-peptide mapping on cellulose thin-layer plates, followed by autoradiography. The radiolabeled peptides were extracted from the cellulose support and immuno-absorbed onto agarose beads carrying a monoclonal antiphosphotyrosine antibody. Next, these beads were transferred to the target disc of the MALDI mass spectrometer, desorbed on target and analyzed. Peptides were identified by their total mass and by their post-source decay (PSD) fragmentation pattern.

Stoichiometry of tyrosyl-phosphorylation

Purified human plasma gelsolin was phosphorylated for 90 min at 37 °C by c-Src (2.5 U) in the presence of a 90-fold molar excess of PIP_2. Whereas 0.036 mol phosphate/mol gelsolin was obtained in the absence of PIP_2, 0.86 mol phosphate/mol gelsolin was measured when gelsolin was incubated with PIP_2. The latter value is much higher then was reported previously (De Corte et al., 1997) and is most likely due to the use of a different batch of [γ^{32}-P]ATP, which was currently obtained from NEN Life Science Products. Previously (De Corte et al., 1997) [γ^{32}-P]ATP was obtained from ICN Biochemicals (Costa Mesa, California). Our recent result indicates that nearly quantitative phosphorylation is achieved, provided only one major site is present in gelsolin.

The HPLC approach

c-Src phosphorylated gelsolin (360 pmol) was digested with trypsin and the resulting peptides separated on a C_4-reverse-phase column. Two major radioactive peaks could be assigned in the UV-absorbency chromatogram (Fig. 1A), containing 92,000 cpm (peak No. 1) and 11,600 cpm (peak No. 2), respectively. Combined, these fractions account for approximately 25% of the total radiolabel present in the unfractionated peptide mixture. Although these recoveries are not low, this moderate value suggested that some other peptides could have been lost, most likely due to insolubility.

ESI-MS spectra recorded for peak No. 1 revealed a mixture of five different peptides (Fig. 1B). The peptide with an observed molecular mass of 3481.8 (±0.1) Da (peptide D in Fig. 1B) likely corresponds with the phosphopeptide I^{425}-R^{454} in accordance with one phosphorylation site (incorporation of one phosphate accounts for 80 Da) since the average mass (M_{av}) of the unphosphorylated peptide was calculated at 3,400.7 Da. The *m/z* (mass to charge ratio) of 871.4 corresponds to the quadruply charged phosphoform of the same peptide, whereas the value of 1,161.6 conforms with the triply protonated phosphoform. The four other peptides with observed molecular masses of: 2,273.1 Da (A^{600}-K^{621}) (peptide A), 2,844.9 Da (N^{368}-R^{392}) (peptide B), 2464.8 Da (V^{276}-K^{300}) (peptide C), and 3,003.8 Da (V^{499}-R^{526}) (peptide E), respectively, correspond with nonphosphogelsolin peptides. Although peak 1 was not homogenous, we were able to confirm the sequence of the phosphopeptide by conventional Edman degradation as I^{425}-R^{454}. Interestingly, while peptide I^{425}-R^{454} produced a minor fraction of ions in the electrospray mode, Edman degradation revealed it was one of the major peptides of the mixture. Peptide I^{425}-R^{454} (^{425}IEGSNKVPVDPATY^{P}GQFYGGDSYIILYNYR^{454}) contains five potential target sites. However, no PTH derivative could be detected in the course of Edman sequencing when the first tyrosine residue was expected. Since the second tyrosine was detected normally (further sequences were not clearly assigned due to the complexity of the mixture), we indirectly concluded that Tyr438 constituted the best candidate for phosphorylation (see below for confirmation).

A similar ESI-MS analysis of peak No. 2 revealed the presence of at least three peptides, one of which showed a derived molecular mass of 2,850.9 (±0.2) Da (peptide A) (see Fig. 1C). This value corresponds with peptide V^{431}-R^{454} covering the same phosphotyrosine but derived by additional cleavage at the Lys430–Val431 bond. The two other peptides correspond with region E^{504}-K^{521} (molecular mass 2,032.9 Da) (peptide B) and region N^{368}-K^{420} (molecular mass 5,702.0 Da) (peptide C).

Thin-layer peptide mapping and phosphopeptide analysis

To avoid the formation of large tryptic phosphopeptides, which could be insoluble during separation on cellulose supports, we now carried out a double digestion, using endoproteinase Lys-C followed by the Asp-N protease. The resulting peptide mixture derived from 180 pmol of phosphogelsolin was separated on cellulose thin-layer plates using a combination of electrophoresis at pH 3.5 followed by a chromatographic step. The phosphopeptide autoradiogram reveals two major spots, labeled 1 and 2 (Fig. 2) and four minor ones, labeled 3–6. It is important to mention that very little radiolabel was detected at the origin of peptide application, which indicates that some insoluble phosphopeptides could be present but in very low amounts.

The radiolabeled peptides were extracted from the cellulose support and recovered by immuno-absorption on agarose-immobilized phosphotyrosine antibodies. The MALDI-TOF spectrum of the desorbed peptide No. 1 is shown in Figure 3A. This spectrum was recorded in the linear mode and was not disturbed by potential contaminants that could have been present in the cellulose matrix or solvents used in the separation procedure. This observation is important because it means that this procedure could be a reliable general approach for phosphotyrosine analysis. The major peak revealed an *m/z* value of 1,550.41 Da corresponding with the phosphorylated peptide V^{431}-G^{444}. The PSD spectrum of this peptide (Fig. 3B) confirmed its identity and provided direct evidence for phosphorylation at position 438. The phosphopeptide V^{431}-

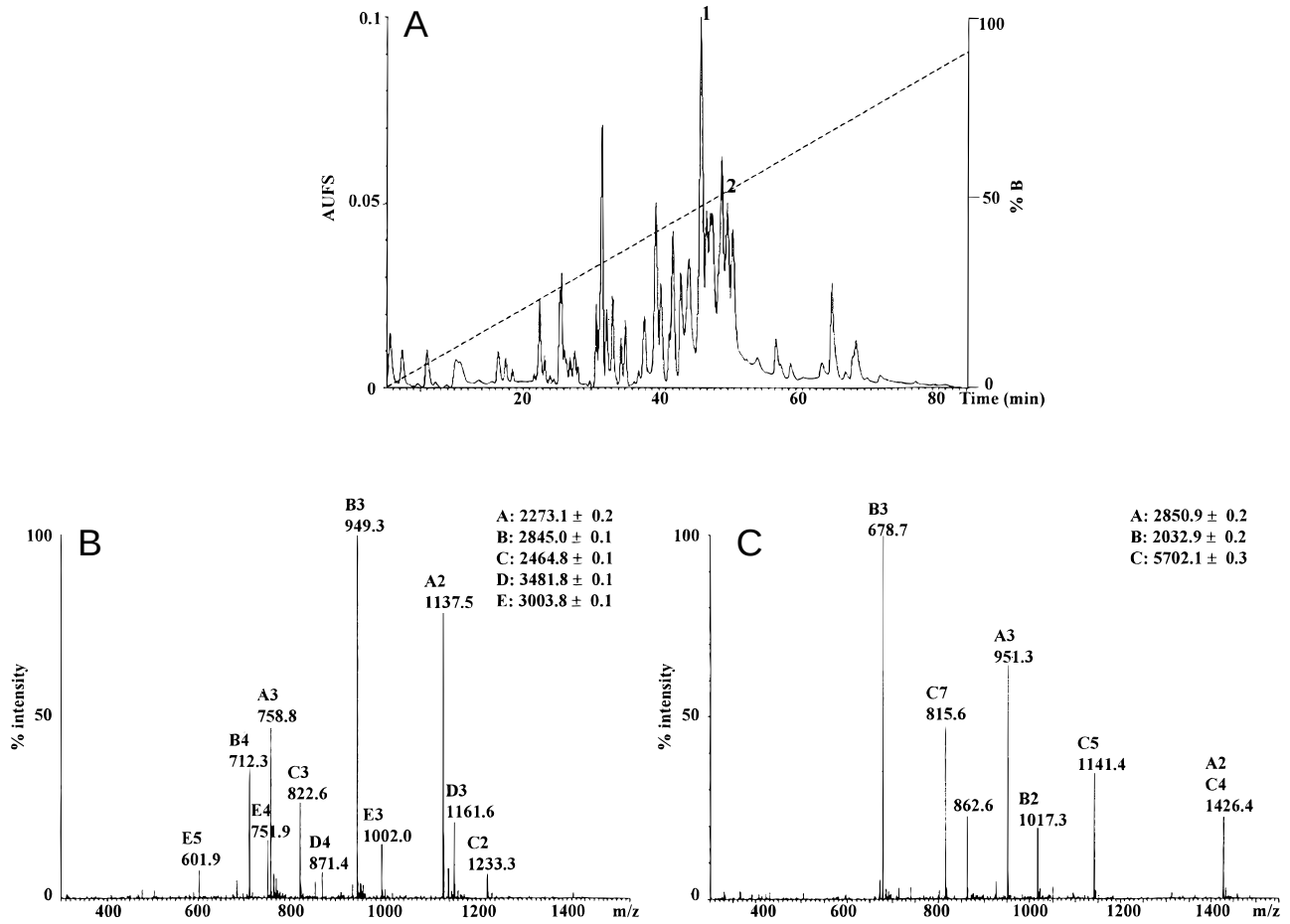

Fig. 1. Separation of ^{32}P-labeled gelsolin tryptic peptides by reverse-phase HPLC followed by ESI-MS analysis of the radioactive peptide peaks. **A:** Narrowbore reverse-phase HPLC chromatogram of the tryptic peptides of phosphorylated gelsolin. The absorbance at 214 nm is shown (———) (AUFS, absorption unit full scale). The dashed line shows the percentage of solution B (acetonitrile in water) (– – – –). Radioactive peptides are numbered 1 and 2. **B:** ESI-MS analysis of radioactive peptide peak 1. The *m/z* (mass to charge ratios) of the peptides are shown on top of the peaks, while the derived molecular weight of the different peptides is shown in the right corner. The *m/z* of 1,161.6 (D3) corresponds to the triply protonated phosphopeptide D. The value of 871.4 (D4) corresponds to the quadruply charged phosphoform. The molecular weight of this phosphopeptide is 3,481.8 (±0.1). **C:** ESI-MS analysis of the radioactive peptide peak 2. The *m/z* values of 1,426.4 (A2) and 951.3 (A3) correspond to the doubly and triply charged phosphopeptide, respectively, which has a derived molecular weight of 2,850.9 (±0.2).

G^{444} migrates during electrophoresis at pH 3.5 with a net charge that is weakly positive, due to full protonation of the α-NH_2 group and poor dissociation of the aspartic acid β-COOH-group and phosphate group.

The second radioactive spot (spot 2) showed streaking during electrophoresis, suggesting limited solubility at low pH. Although it represents approximately one-third of the total radiolabel of the original peptide mixture, it is most likely not a (phospho)peptide because: (1) no radiolabel was absorbed by the agarose-bound antibodies, while nearly 100% was absorbed for spot 1; (2) when phosphoamino acid analysis was performed, no radioactivity was found to comigrate with phosphoamino acids (data not shown); (3) the same spot with unchanged characteristic chromatographic behavior was also observed when other proteases, such as trypsin or thermolysin, were used (data not shown). Taken together, the TLC-MALDI approach confirms our previous conclusion for a major phosphorylation site at Tyr438, while additional sites may be present (see minor spots labeled 3, 4, 5, and 6) though at much lower amounts.

Identification of the minor phosphorylation sites in gelsolin

To identify the minor phosphorylation sites in the c-Src phosphorylated gelsolin (Fig. 2), phosphogelsolin was digested with endo-Lys-C, and phosphopeptides were immediately immunoprecipitated with the anti-phosphotyrosine agarose and analyzed by MALDI-MS and subsequent PSD analysis, without an intermediary TLC purification step. Five peaks were observed, corresponding with four different phosphopeptides (Fig. 4). Notice the low signal to noise ratio, indicating low yield recoveries of minor phosphorylation sites. PSD analysis could be performed on three of these peptides, allowing their identification (results not shown). The peptide with a mass of 1,242.9 Da most likely corresponds with the A^{622}-K^{631} sequence containing one phosphotyrosine (Tyr624). The amino acid sequences of the additional phosphopeptides are shown in Figure 4 revealing minor phosphorylation sites at Tyr59, Tyr382, and Tyr576, respectively. The phosphopeptide corresponding with the major Tyr438 site is not present in this spectrum because it is expected to appear in a peptide with a predicted high mass (8,022.9 Da) not

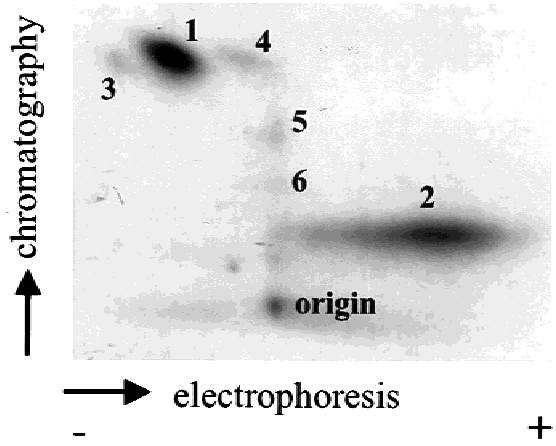

Fig. 2. Phosphopeptide map of ^{32}P-labeled gelsolin, subsequently digested with endoproteinases Lys-C and Asp-N. The peptides were resolved by electrophoresis at pH 3.5 in the horizontal dimension and by ascending chromatography in the second dimension. The autoradiogram was exposed overnight at −80 °C. The positions of the radioactive spots (1–6) are shown. The origin of application is also indicated. The cathode (−) and anode (+) positions are shown.

covered by this analysis. However, when phosphogelsolin was digested with trypsin, the phosphopeptide (I^{425}-R^{454}), with a derived molecular mass of 3,479.88 Da, was identified by direct MALDI analysis (data not shown). In this experiment an additional, weakly ionizing phosphopeptide, was also found corresponding with the doubly phosphorylated I^{425}-R^{454} phosphopeptide (3,560.01 Da). We do not know which of the four other tyrosine residues next to Tyr438 is phosphorylated because no PSD data could be collected.

These additional phosphorylation sites account for only a marginal percentage of incorporated phosphate and are far below the degree of phosphorylation observed in Tyr438. We looked back to the ESI-MS profile and only in the case of Tyr382 there was a weak indication for the presence of the corresponding phosphopeptide.

Antibodies specific to the pho438 region recognize gelsolin phosphorylated by c-Src in the absence of phospholipids or after stimulation with LPA or PIP_2

Human plasma gelsolin phosphorylation by c-Src was carried out in the presence of PIP_2 as activator. The conditions used resulted in a near stoichiometric modification at residue Tyr438. When the same experiments were carried out in the presence of lysophosphatidic acid as activator (which binds to several actin-binding proteins of the gelsolin family), we observed phosphorylation of the same site. A chemically synthesized phosphotyrosine peptide, covering the region around Tyr438 was coupled via an NH_2-terminal cysteine residue onto keyhole limpet haemocyanin and used to immunize rabbits. As shown in Figure 5 (lanes a and b), the anti-phosphopeptide antibodies specifically recognize c-Src-phosphorylated gelsolin preincubated with LPA, while the unphosphorylated form was not detected. In the absence of any activating compounds, partial phosphorylation was also detected at this residue. This was substantiated with the anti-phosphotyrosine-MALDI approach (data not shown) and confirmed by Western blot analysis (Fig. 5, lanes c2 and d2). A polyclonal antibody against gelsolin was used as an internal control (lanes c1 and d1)

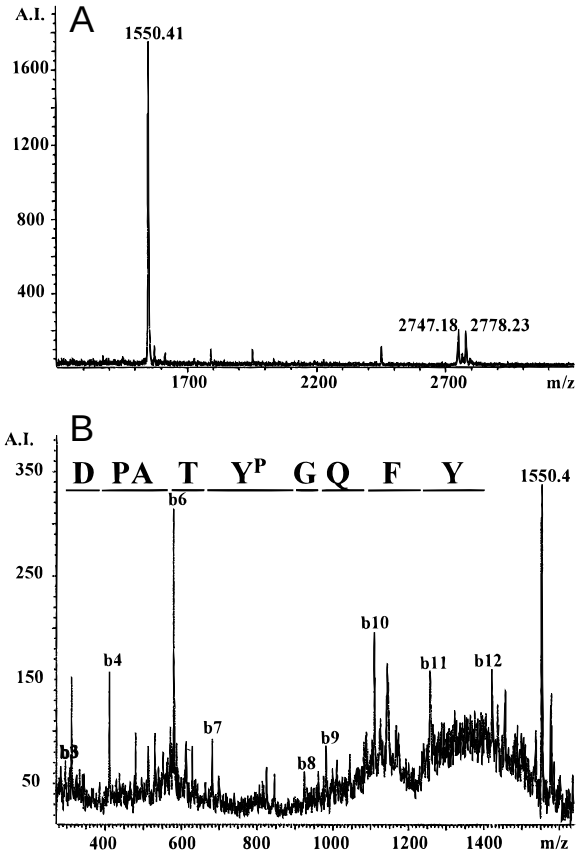

Fig. 3. MALDI-MS analysis of spot 1. **A:** MALDI-MS spectrum of spot 1 (see Fig. 2). Cellulose was scraped off the plate, the phosphopeptide was eluted in Tris-buffer and incubated with anti-phosphotyrosine-coupled agarose. The 2,747.18 and 2,778.23 Da peaks theoretically do not correspond with gelsolin peptides and further identification was unsuccessful. **B:** MALDI-PSD spectrum of the 1,550.41 Da peptide. The b-ions are indicated. The matching sequence of the phosphopeptide is shown. A.I. = absolute intensity.

Finally, we also studied phosphorylation of human recombinant cytosolic gelsolin and identified the same target tyrosine residue. The phosphorylation was limited in the absence of phospholipids, as for plasma gelsolin, but was highly stimulated in the presence of PIP_2 and LPA (data not shown). These studies indicate that there is no difference in c-Src phosphorylation between the secreted and cytosolic forms of gelsolin with respect to the tyrosine target site and the stimulation by PIP_2 or LPA.

Phosphorylation of gelsolin in the gelsolin-actin dimer or the gelsolin-$actin_2$ trimer complexes

To investigate the possible role of gelsolin phosphorylation on actin-binding, we reconstituted 1:1 and 1:2 complexes between gelsolin and muscle actin and subsequently phosphorylated gelsolin by c-Src (in the absence of phospholipids). Gelsolin (2.5 μM) was incubated with actin (2.5 or 5 μM) in the presence of 0.2 mM Ca^{2+}. After 2 h incubation at 4 °C, the complexes were phosphorylated with c-Src for 90 min and analyzed by SDS-PAGE (10%) and autoradiography (see Fig. 6). The gelsolin-actin dimer was less efficiently phosphorylated (50% inhibition in comparison to gelso-

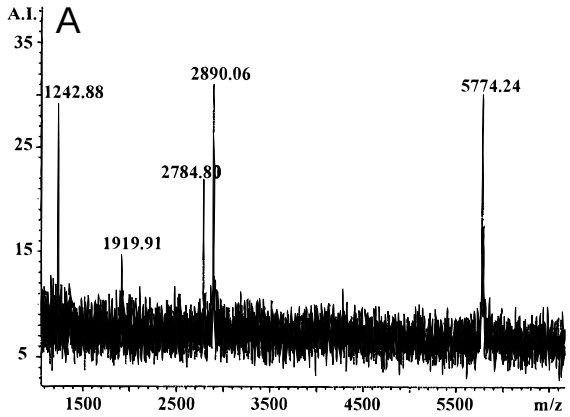

Mass (Da)	PSD	Phosphopeptide
1242.9	-	^{622}AAY^{p}RTSPRLK^{631}
1919.9	+	^{571}TPSAAY^{p}LWVGTGASEAEK^{588}
2784.8	+	^{49}FDLVPVPTNLY^{p}GDFFTGDAYVILK^{72}
5774.2	+	^{368}NWRDPDQTDGLGLSY^{p}LSSHIANVERVP FDAATLHTSTAMAAQHGMDDDGTGQK^{420}

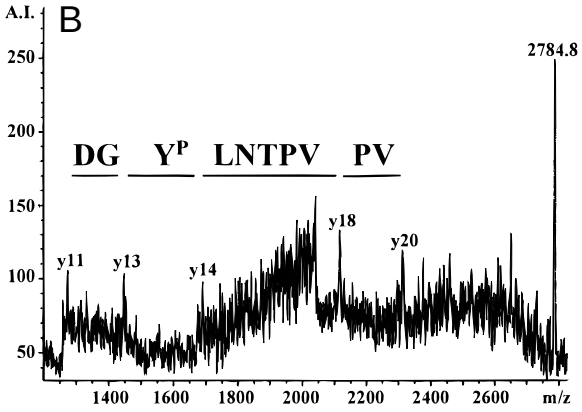

Fig. 4. MALDI-MS spectrum of phosphorylated gelsolin peptides. **A:** Phosphogelsolin was digested with endoproteinase Lys-C, incubated with the anti-phosphotyrosine-coupled agarose beads and analyzed by MALDI-MS. The masses corresponding to the phosphotyrosine peptides are indicated. The phosphopeptide with a mass of 2,890.06 Da corresponds with the doubly charged 5,774.24 Da phosphopeptide. A.I. = absolute intensity. The sequences of the phosphopeptides corresponding with the minor sites are shown below. **B:** MALDI-PSD spectrum of the 2,784.8 Da peptide. The y-ions are indicated and the matching sequence of the phosphorylated peptide is shown.

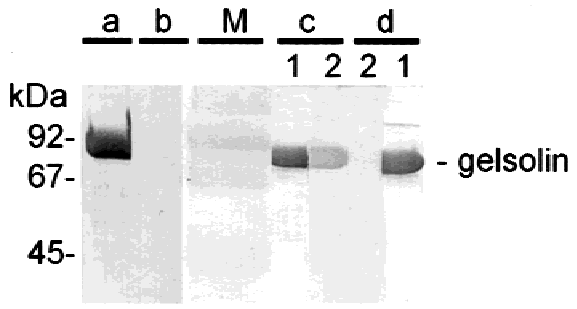

Fig. 5. Antibodies raised against the pho438 gelsolin peptide specifically recognize c-Src phosphorylated gelsolin. **a:** Phosphorylation of gelsolin preincubated with LPA and probed with antibodies specific for phospho-438-gelsolin. **b:** Unphosphorylated gelsolin (control) probed with the same antibodies. **c:** Phosphorylation of gelsolin in the absence of phospholipid; the lane was cut in two and then probed with either polyclonal gelsolin antibodies (lane 1) or pho438-gelsolin antibodies (lane 2). **d:** Unphosphorylated gelsolin; lane d was also cut in two and probed with the same antibodies as described in (**c**). M = Molecular weight markers (92, 67, and 45 kDa are shown).

lin alone), whereas phosphorylation of the gelsolin-actin$_2$ trimer was almost completely inhibited (90% inhibition). The addition of EGTA (2.5 mM) to the gelsolin-actin$_2$ trimer (to reconstitute the EGTA resistant gelsolin-actin dimer) restores phosphorylation of gelsolin comparable to phosphorylation in the 1/1 complex.

Discussion

The present study strives to understand in more detail the biological role of the PIP$_2$- and LPA-activated c-Src phosphorylation of a number of actin-binding proteins, in particular of gelsolin. Toward this aim we determined the main tyrosine target residue in gelsolin. The initial experiments were carried out with human plasma gelsolin, but identical results were also obtained with the human recombinant cytosolic isoform.

For these studies we used two complementary protein chemical approaches. One was based on the conventional HPLC-ESI-MS (Fenn et al., 1989) combination, while the second approach involved thin-layer peptide mapping followed by phosphotyrosine-specific immuno-absorption (Zhao & Chait, 1994), MALDI-TOF-MS (Karas & Hillenkamp, 1988), and PSD analysis (Spengler et al., 1992). TLC-peptide mapping provided direct visualization of all phosphopeptides, revealing possible remaining phosphorylated peptides at the origin of application. Such peptides are insoluble and therefore mostly overlooked in conventional HPLC analysis. Our present data showed that very little radioactivity was present at the origin of application (Fig. 2). Interestingly, our MALDI measurements were not disturbed by possible contaminants originating from the cellulose or solvents, indicating this strategy was selective and efficient.

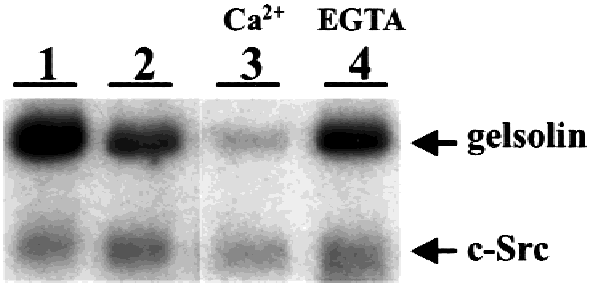

Fig. 6. Gelsolin phosphorylation in the gelsolin-actin and gelsolin-actin$_2$ complexes. Gelsolin (2.5 μM) was incubated for 90 min at 37 °C with the appropriate amounts of G-actin in the presence of 0.2 mM Ca^{2+} and then phosphorylated with c-Src in the absence of phospholipids. Lane 1: control (gelsolin alone); lane 2: G/A complex; lane 3: G/A$_2$ complex; lane 4: G/A$_2$ complex incubated with EGTA corresponding to the G/A complex. The film was exposed for 60 h at −80 °C.

The major target Tyr438 is located within a highly conserved region of the gelsolin sequence in segment S4 (overlapping Gln419 to Leu511) (Burtnick et al., 1997). Although the exact binding site of G-actin to gelsolin S4 is not known (Pope et al., 1995), it has been postulated, based on the sequence homology between S1 and S4 of gelsolin, that the α helix in S4 (residues Gln473–Glu488) could also be important for actin-binding (Pope et al., 1995). Because Tyr438 is located outside the presumed actin-binding site, we hypothesize that the inhibition of phosphorylation of the gelsolin-$actin_2$ trimer is due to sterical hindrance.

To identify the minor phosphorylation sites, we also used the more direct anti-phosphotyrosine immuno-absorption approach (Zhao & Chait, 1994), starting from the complete peptide mixture, followed by MALDI mass spectrometry and PSD analysis. We were able to identify at least four additional, but minor, c-Src target sites (Tyr59, Tyr382, Tyr576, and Tyr624). These minor sites most likely would have escaped detection by other methods. Their identification illustrates the high sensitivity of the MALDI-MS approach even starting from nonradioactive material.

Src is suggested to play a role in the organization of focal adhesions mediated by integrin receptors and several of these components are substrates of v-Src including paxillin (Richardson et al., 1997), $p130^{cas}$ (Petch et al., 1995), talin (Pasquale et al., 1986; DeClue & Martin, 1987), tensin (Davis et al., 1991), vinculin (Sefton et al., 1981), and FAK (Schlaepfer & Hunter, 1996). v-Src also induces membrane ruffling and lamellipodia in cells with PI-3 kinase (Haefner et al., 1995), ezrin (Krieg & Hunter, 1992), cortactin (Huang et al., 1997), and $p190Rho^{GAP}$ (Ellis et al., 1990; Bouton et al., 1991) as substrates.

So far in vivo phosphorylation of gelsolin by Src has escaped detection. Our in vitro data show a very strong stimulation of phosphorylation only in the presence of PIP_2 or LPA. It was also demonstrated that PIP_2 does not act directly as an activator of c-Src, but rather that gelsolin is turned into a better substrate when interacting with the phospholipids. Other reports have pointed to effects of PIP_2 on gelsolin function. For instance, in vitro studies have shown that gelsolin modulates the activity of several important signaling enzymes through interactions with PIP_2. This is the case for the phosphoinositide-specific phospholipase C (Banno et al., 1992; Baldassare et al., 1997; Sun et al., 1997) and phospholipase D (Liscovitch et al., 1994; Steed et al., 1996). Recently Chellaiah et al. (1998) showed that osteopontin stimulates association between gelsolin and c-Src, leading to increased gelsolin-associated PI-3 kinase activity and PIP_3 levels in osteoclasts. This shows that both components temporarily interact in vivo under particular circumstances and that possibly under these or similar conditions gelsolin phosphorylation may occur.

Having the antibodies, which are specific for gelsolin and pho438-gelsolin, at our disposal, we are in a position to begin an extensive screening study in identifying cellular systems in which this event happens and in locating phosphogelsolin inside the cell.

Materials and methods

Materials

The [γ-^{32}P]ATP (3,000 Ci/mmol) was from NEN Life Science Products (Boston, Massachusetts). Anti-phosphotyrosine-agarose (clone PT66), keyhole limpet hemocyanin, and $H_2{}^{18}O$ were obtained from Sigma (St. Louis, Missouri). Trypsin, endoproteinase Asp-N, and endoproteinase Lys-C (sequencing grade) were from Boehringer (Mannheim, Germany). α-Cyano-4-hydroxycinnamic acid, purchased from Sigma, was recrystallized in ethanol prior to use whereas 2,5-dihydroxybenzoic acid (Fluka, Buchs, Switzerland) was used without further purification.

Proteins and lipids

Gelsolin was purified from human plasma according to Cooper et al. (1987). Recombinant human cytosolic gelsolin (pET11-gelsolin vector transformed in *Escherichia coli* pSCM-26 strain (Mertens et al., 1995)) was kindly provided by K. Meerschaert (Department of Biochemistry, University Gent, Belgium). Rabbit skeletal muscle actin was prepared according to established procedures (Spudich & Watt, 1971) and isolated as Ca^{2+}-G-actin by chromatography over Sephadex G200 in G-buffer (5 mM Tris/HCl pH 7.7, 0.2 mM ATP, 0.5 mM 2-mercaptoethanol, 0.2 mM $CaCl_2$, and 0.02% NaN_3). Recombinant human c-Src kinase had a specific activity of 900,000 U/mg and was obtained from Upstate Biotechnology Incorporated (New York, New York).

PIP_2 and LPA from Sigma were dissolved in water (5 mM final concentration). PIP_2 was sonicated for 30 min in a Branson S75 sonicator (Branson Sonic Power Co., Danbury, Connecticut) and stored in aliquots at $-80\,^{\circ}C$. Before use PIP_2 was sonicated for an additional 5 min.

Phosphorylation assays and immunoprecipitation of tyrosine-phosphorylated peptides

Reactions were performed as described previously (De Corte et al., 1997). Briefly, gelsolin (2.5 μM) was phosphorylated with 2.5 U c-Src at 30 °C for 90 min with or without PIP_2 or LPA (used at 225 μM) in a total volume of 12.5 μL containing 10 mM Tris/HCl pH 7.5, 10 mM $MgCl_2$, 100 μM ATP, and 1 mM DTT. [γ-^{32}P] ATP had a specific radioactivity of 1,000–1,500 cpm/pmol. After phosphorylation the samples were boiled for 3 min and cooled on ice. Trypsine (1:40 w/w) was added together with 10 μL of a 30 mM Tris/HCl pH 8.0 solution. Alternatively, endo-Lys-C (1:40 w/w) and 1.5 μL of a 10 $\times$ concentrated solution (250 mM Tris/HCl pH 8.5, 10 mM EDTA) were added. In both cases the digestion was allowed to proceed for 4 h at 37 °C. The proteases were denaturated by boiling the sample for 5 min and in the case of trypsin, trypsin inhibitor from Sigma was added in a 2.5 excess (w/w) over trypsin. The following procedure is largely based on the one described by Zhao and Chait (1994). Anti-phosphotyrosine (clone PT66) coupled agarose was added (5 μL suspension) and the mixture was incubated overnight at 4 °C with constant end over end rotation. The beads were washed with 1 mL 10 mM Tris/HCl, pH 7.5 supplemented with 200 mM NaCl and centrifuged briefly at 2,200 rpm. The washing step was repeated four times and the beads were finally washed twice with 1 mL of water.

Reverse-phase HPLC analysis of phosphogelsolin

Phosphogelsolin (360 pmol) was dialyzed overnight at 4 °C to remove excess radioactive ATP. The sample was boiled and digested with trypsin (1:40 w/w) for 4 h at 37 °C and the resulting peptides were separated on a narrowbore C_4 reverse-phase column (2.1 $\times$ 50 mm) connected to a 140A HPLC instrument from Applied Biosystems Inc. (Foster City, California). The column was equilibrated in 0.1% trifluoroacetic acid (TFA) and proteins were eluted with a linear gradient of 0 to 90% acetonitrile in 0.1% TFA

at a flow rate of 80 μL/min. Radioactive peptides were monitored by Cerenkov radiation and analyzed by amino acid sequencing and ESI-MS analysis. Details with regard to the ESI-MS analysis can be found in De Corte et al. (1996). Amino acid sequence analysis was performed with a 477A model pulsed liquid-phase sequenator equipped with a 120A phenylthiohydantoin amino acid analyzer from Applied Biosystems Inc.

Two-dimensional phospho-peptide mapping

Gelsolin (180 pmol) was phosphorylated as described above and further purified by reverse-phase HPLC. A C_{18} column (4.6 $\times$ 210 mm, 5 μm particle size, 300 Å pore size; Vydac, Separations Group, Hesperia, California) was equilibrated in 0.1% trifluoroacetic acid (TFA) and the protein was eluted using a linear gradient of 0 to 90% acetonitrile at a flow rate of 1 mL/min. The gradient was started 5 min after sample loading and finished after 70 min. The phosphorylated gelsolin was Speed Vac dried, resuspended in 60 mM NH_4HCO_3, pH 8.0, and digested with endo-Lys-C (1:40 w/w) for 4 h at 37 °C, boiled for 3 min to denature the protease and subsequently digested with Asp-N (1:40 w/w) overnight at 37 °C, and finally boiled again. The resulting peptides were labeled at their C-terminus by the incorporation of ^{18}O atoms as previously described (Takao et al., 1993; Gevaert et al., 1997). The sample was lyophilized and dissolved in electrophoresis buffer consisting of glacial acetic acid/pyridin/water (50/5/945; v/v, pH 3.5). It was applied onto a cellulose plate (20 $\times$ 20 cm) (Merck, Darmstadt, Germany) and subjected to electrophoresis for 3 h at 400 V making use of the Multiphor II horizontal electrophoresis unit (Pharmacia Biotech, Brussels, Belgium). The second dimension was a chromatography step, run in 1-butanol/pyridin/glacial acetic acid/water (75/50/15/60; v/v). The radioactive peptides were visualized by autoradiography and the cellulose corresponding to the radioactive spots was scraped off and eluted in 20 mM Tris/HCl pH 7.5 by continuous shaking at room temperature. After 30 min the samples were centrifuged for 5 min at 12,000 rpm. More than 90% of the radioactivity was recovered in the supernatant, which was subsequently incubated overnight at 4 °C with anti-phosphotyrosine coupled agarose as described above.

MALDI-MS

A concentrated MALDI-matrix solution was prepared by mixing 20 mg α-cyano-4-hydroxycinnamic acid and 4 mg 2,5-dihydroxybenzoic acid in 500 μL 0.1% TFA in 50% acetonitrile/water. This solution was diluted fivefold with 0.1% TFA in 50% acetonitrile/water prior to each MALDI-MS experiment. Two microliters of the diluted matrix solution was mixed with the dried peptide-bound anti-phosphotyrosine agarose beads. Subsequently, 0.5 μL was transferred to the MALDI-target and allowed to air-dry. All MALDI mass spectra were recorded with an upgraded Bruker Reflex III Instrument (Bruker-Franzen Analytik GmbH, Bremen, Germany) using the delayed extraction mode (Colby et al., 1994). Ionization was achieved using a nitrogen laser (337 nm beam, 3 ns pulse width, 5 Hz) set at an attenuation between 35–55. Running parameters were optimized for the different types of measurements. For linear and reflectron measurements the instrument was externally calibrated using the monoisotopic masses of Angiotensin II (Sigma) and of the adrenocorticotropic hormone ACTH 18–39 clip (Sigma). For PSD measurements, the instrument was calibrated using the known fragment masses of the ACTH 18–39 clip. Prior to PSD analysis, the peptide of interest was separated from other peptides in the linear spectrum using a timed pulse of 700 V with the FastPulse^{MT} option. PSD spectra were acquired in 10–14 segments (each being the average of 50–100 spectra), with each segment representing a 25% decrease in reflectron voltage. The spectra shown here are the result of the accumulation into a contiguous PSD spectrum using the Bruker FAST^{TM} software.

Peptide synthesis and generation of antibodies

The gelsolin phosphopeptide with the sequence NH_2·CKVPVDP ATY$^{\mathbf{P}}$GQFYGGDS·OH was synthesized with a 431A automated peptide synthesizer from Applied Biosystems. The synthesis was done using the Fmoc (fluoren-9-ylmethoxycarbonyl) chemistry procedure following the manufacturer's instructions. The Fmoc-Tyr(PO(OBzl)-OH)-OH (N-α-Fmoc-O-benzyl-L-phosphotyrosine) was obtained from Calbiochem-Novabiochem AG (Läufelfingen, Switzerland). All other amino acid derivatives were obtained from Advanced Chemtech (Louisville, Kentucky). This phosphopeptide was coupled to KLH (keyhole limpet hemocyanin) according to Mumby and Gilman (1991). The phosphopeptide was cleaved from the resin with TFA and desalted in water over a G-25 column (30 $\times$ 2.6 cm), further purified by preparative HPLC on a 1 $\times$ 25 cm C_4 reverse-phase column (Vydac, Separations Group, Hesperia, California), desalted as above, and stored in lyophilized form at -20 °C. The correct mass of the phosphopeptide was determined by ESI-MS.

The KLH-coupled phosphopeptide (500 μg) or plasma gelsolin (150 μg) (obtained by reverse-phase HPLC) were emulsified in Freund's complete adjuvant and injected subcutaneously. Twenty-four days after the initial immunization, the rabbit was again injected with 500 μg of the peptide or 150 μg of gelsolin in Freund's incomplete adjuvant. The booster injection was repeated on day 45. After 66 days the rabbit was bled and serum was prepared. The anti-gelsolin immunoglobulins were purified by affinity chromatography as described in Gettemans et al. (1995).

Miscellaneous

Protein concentrations were determined by the method of Bradford (1976) using bovine serum albumin as standard. SDS-polyacrylamide gel electrophoresis was carried out according to Matsudaira and Burgess (1978). Western blot analysis was performed as described by Towbin et al. (1979).

Acknowledgments

This work was supported by grants from the Fund for Scientific Research-Flanders (Belgium) (F.W.O.) and by the Interuniversity Attraction Poles to J.V. (IUAP/PIV/23, Federal Services for Science, Technology and Culture Affairs). J.G. is a Postdoctoral Fellow of the Fund for Scientific Research-Flanders (Belgium) (F.W.O.).

References

Baldassare JJ, Henderson PA, Tarver A, Fisher GJ. 1997. Thrombin activation of human platelets dissociates a complex containing gelsolin and actin from phosphatidylinositide-specific phospholipase Cgamma1. *Biochem J 324*:283–287.

Banno Y, Nakashima T, Kumada T, Ebisawa K, Nonomura Y, Nozawa Y. 1992. Effects of gelsolin on human platelet cytosolic phosphoinositide-phospholipase C isozymes. *J Biol Chem 267*:6488–6494.

Bouton AH, Kanner SB, Vines RR, Wang HC, Gibbs JB, Parsons JT. 1991. Transformation by pp60$^{c\text{-}src}$ or stimulation of cells with epidermal growth factor induces the stable association of tyrosine-phosphorylated cellular proteins with GTPase-activating protein. *Mol Cell Biol 11*:945–953.

Bradford MM. 1976. A rapid and sensitive method for the quantification of microgram quantities of protein utilizing the principle of protein-dye binding. *Anal Biochem 72*:248–254.

Bretscher A, Weber K. 1979. Villin: The major microfilament associated protein of the intestinal microvillus. *Proc Natl Acad Sci USA 76*:2321–2325.

Burtnick LD, Koepf EK, Grimes J, Jones EY, Stuart DI, McLaughlin PJ, Robinson RC. 1997. The crystal structure of plasma gelsolin: Implications for actin severing, capping, and nucleation. *Cell 90*:661–670.

Chellaiah M, Fitzgerald C, Alvarez U, Hruska K. 1998. c-Src is required for stimulation of gelsolin associated phosphatidylinositol 3-kinase. *J Biol Chem 273*:11908–11916.

Colby S, King T, Reilly J. 1994. Improving the resolution of matrix assisted laser desorption/ionization time-of-flight mass spectrometry by exploiting the correlation between ion position and velocity. *Rapid Commun Mass Spectrom 8*:865–873.

Cooper JA, Bryan J, Schwab B III, Frieden C, Loftus DJ, Elson EL. 1987. Microinjection of gelsolin into living cells. *J Cell Biol 104*:491–501.

Davis S, Lu ML, Lo SH, Lin S, Butler JA, Druker BJ, Roberts TM, An Q, Chen LB. 1991. Presence of an SH2 domain in the actin-binding protein tensin. *Science 252*:712–715.

DeClue JE, Martin GS. 1987. Phosphorylation of talin at tyrosine in Rous sarcoma virus transformed cells. *Mol Cell Biol 7*:371–378.

De Corte V, Gettemans J, De Ville Y, Waelkens E, Vandekerckhove J. 1996. Fragmin, a microfilament regulatory protein from *Physarum polycephalum*, is phosphorylated by casein kinase II type enzymes. *Biochemistry 35*:5472–5480.

De Corte V, Gettemans J, Vandekerckhove J. 1997. Phosphatidyl 4,5-bisphosphate specifically stimulates pp60$^{c\text{-}src}$ catalyzed phosphorylation of gelsolin and related actin-binding proteins. *FEBS Lett 401*:191–196.

Ellis C, Moran M, McCormick F, Pawson T. 1990. Phosphorylation of GAP and GAP associated proteins by transforming and mitogenic tyrosine kinases. *Nature 343*:377–381.

Fenn J, Mann M, Meng C, Wong S. 1989. Electrospray ionization for mass spectrometry of large biomolecules. *Science 246*:64–71.

Gettemans J, De Ville Y, Waelkens E, Vandekerckhove J. 1995. The actin-binding properties of the *Physarum* actin-fragmin complex. *J Biol Chem 270*:2644–2651.

Gevaert K, De Mol H, Verschelde JL, Van Damme J, De Boeck S, Vandekerckhove J. 1997. Novel techniques for identification and characterization of proteins loaded on gels in femtomole amounts. *J Protein Chem 16*:335–342.

Haefner B, Baxter R, Fincham VJ, Downs CP, Frame MC. 1995. Cooperation of Src homology domains in the regulated binding of phosphatidylinositol 3-kinase. A role for the Src homology 2 domain. *J Biol Chem 270*:7937–7943.

Hartwig JH, Bokoch GM, Carpenter CL, Janmey PA, Taylor LA, Toker A, Stossel TP. 1995. Thrombin receptor ligation and activated rac uncap actin filament barbed ends through phosphoinositide synthesis in permeabilized human platelets. *Cell 82*:643–653.

Huang C, Ni Y, Wang T, Gao Y, Haudenschild CC, Zhan X. 1997. Down regulation of the filamentous actin crosslinking activity of cortactin by src mediated tyrosine phosphorylation. *J Biol Chem 272*:13911–13915.

Janmey PA, Chaponnier C, Lind SE, Zaner KS, Stossel TP, Yin HL. 1985. Interactions of gelsolin and gelsolin-actin complexes with actin. Effects of calcium on actin nucleation, filament severing, and end blocking. *Biochemistry 24*:3714–3723.

Janmey PA, Stossel TP. 1987. Modulation of gelsolin function by phosphatidyl 4,5-bisphosphate. *Nature 325*:362–364.

Karas M, Hillenkamp F. 1988. Laser desorption ionization of proteins with molecular masses exceeding 10,000 daltons. *Anal Chem 60*:2299–2301.

Krieg J, Hunter T. 1992. Identification of the two major epidermal growth-factor induced tyrosine phosphorylation sites in the microvillar core protein ezrin. *J Biol Chem 267*:19258–19265.

Liscovitch M, Chalifa V, Pertile P, Chen CS, Cantley LC. 1994. Novel function of phosphatidylinositol 4,5-bisphosphate as a cofactor for brain membrane phospholipase D. *J Biol Chem 269*:21403–21406.

Maekawa S, Toriyama M, Hisanaga S, Yonezawa N, Endo S, Hirokawa N, Sakai H. 1989. Purification and characterization of a Ca^{2+} dependent actin filament severing protein from bovine adrenal medulla. *J Biol Chem 264*:7458–7465.

Matsudaira PT, Burgess DR. 1978. SDS microslab linear gradient polyacrylamide gel electrophoresis. *Anal Chem 87*:386–396.

Meerschaert K, De Corte V, De Ville Y, Vandekerckhove J, Gettemans J. 1998. Gelsolin and functionally similar actin-binding proteins are regulated by lysophosphatidic acid. *EMBO J 17*:5923–5932.

Mertens N, Remaut E, Fiers W. 1995. Tight transcriptional control mechanism ensures stable high level expression from T7 promotor based expression plasmids. *Bio Technol 13*:175–179.

Moolenaar WH, Kranenburg O, Postma FR, Zondag GCM. 1997. Lysophosphatidic acid: G-protein signaling and cellular responses. *Curr Opin Cell Biol 9*:168–173.

Mumby SM, Gilman AG. 1991. Synthetic peptide antisera with determined specificity for G protein alpha or beta subunits. *Methods Enzymol 195*:215–233.

Pasquale EB, Maher PA, Singer SJ. 1986. Talin is phosphorylated on tyrosine in chicken embryo fibroblasts transformed by Rous sarcoma virus. *Proc Natl Acad Sci USA 83*:5507–5511.

Petch LA, Bockholt SM, Bouton A, Parsons JT, Burridge K. 1995. Adhesion induced tyrosine phosphorylation of the p130 src substrate. *J Cell Sci 108*:1371–1379.

Pope BJ, Gooch JT, Weeds AG. 1995. Localization of Ca^{2+} sensitive actin monomer binding sites in gelsolin to segment-4 and identification of calcium binding sites. *Biochemistry 34*:1583–1588.

Richardson A, Malik RK, Hildebrand JD, Parsons JT. 1997. Inhibition of cell spreading by expression of the C-terminal domain of focal adhesion kinase (FAK) is rescued by coexpression of Scr or catalytically inactive FAK: A role for paxillin tyrosine phosphorylation. *Mol Cell Biol 17*:6906–6914.

Schlaepfer DD, Hunter T. 1996. Evidence for in vivo phosphorylation of the Grb2 SH2-domain binding site on focal adhesion kinase by Src family protein-tyrosine kinases. *Mol Cell Biol 16*:5623–5633.

Sefton BM, Hunter T, Bal EH, Singer SJ. 1981. Vinculin: A cytoskeletal target of the transforming protein Rous sarcoma virus. *Cell 24*:165–174.

Spengler B, Kirsch D, Kaufmann R, Jaeger E. 1992. Peptide sequencing by matrix assisted laser desorption mass spectrometry. *Rapid Commun Mass Spectrom 6*:105–108.

Spudich JA, Watt S. 1971. The regulation of rabbit skeletal muscle contraction. *J Biol Chem 246*:4866–4871.

Steed PM, Nagar S, Wennogle LP. 1996. Phospholipase D regulation by a physical interaction with the actin-binding protein gelsolin. *Biochemistry 35*:5229–5237.

Sun HQ, Lin KM, Yin HL. 1997. Gelsolin modulates phospholipase C activity in vivo through phospholipid binding. *J Cell Biol 138*:811–820.

Takao T, Gonzalez J, Yoshidome K, Sato K, Asada T, Kammei Y, Shimonishi Y. 1993. Automatic precursor-ion switching in a four-sector tandem mass spectrometer and its application to acquisition of the MS/MS product ions derived from a partially (18)O-labeled peptide for their facile assignments. *Anal Chem 65*:2394–2399.

Towbin H, Staehelin T, Gordon J. 1979. Electrophoretic transfer of proteins from polyacrylamide gels to nitrocellulose sheets: Procedure and some applications. *Proc Natl Acad Sci USA 76*:4350–4354.

Vandekerckhove J. 1990. Actin-binding proteins. *Curr Opin Cell Biol 2*:41–50.

Zhao Y, Chait BT. 1994. Protein epitope mapping by mass spectrometry. *Anal Chem 66*:3723–3726.